Available online at www.sciencedirect.com
ScienceDirect
Sensors and Actuators A 133 (2007) 96–103
SENSORS AND ACTUATORS A PHYSICAL
www.elsevier.com/locate/sna

Reduction of blind zone in ultrasonic transmitter/receiver transducers

Álvaro Hernández [a,*], Jesús Ureña [a], Manuel Mazo [a], Juan J. García [a], Ana Jiménez [a], Fernando J. Álvarez [b]

[a] *Electronics Department, University of Alcalá, Campus Universitario s/n, E-28806, Alcalá de Henares, Madrid, Spain*
[b] *Department of Electronics and Electromechanical Engineering, University of Extremadura, Cáceres, Spain*

Received 8 September 2005; received in revised form 10 March 2006; accepted 14 March 2006
Available online 21 April 2006

Abstract

Most ultrasonic sensorial systems are based on transducers that work as emitters and receivers in the same scanning process. This fact implies that, during the emission process, the reception stage stays disabled, in order to avoid the emission coupled. This disabling interval provides that the nearest area to the transducers, the blind zone, cannot be scanned, since echoes coming from reflectors placed inside it are overlapped with the coupled emission. On the other hand, the encoding of the ultrasonic emission by binary sequences allows the process gain to be increased, so better precision is achieved and higher levels of noise are supported by the system. The length of the used binary sequence determines not only the process gain, but also the duration of the emission interval. The usage of long sequences to improve the performance also implies the existence of a larger blind zone, where reflectors are not detected. This work presents a novel encoding technique, based on Golay complementary pairs, where the dimension of the blind zone is reduced to negligible distances thanks to some features from the binary sequences.

Keywords: Ultrasonic transducer; Encoded ultrasonic emission; Blind zone; Golay complementary pair

1. Introduction

Ultrasonic sensorial systems have been installed on mobile robots for a long time [1,2]. Trying to take advantage of their simplicity, these systems are usually based on transducers with the capability of emission and reception [3–7]. The time-of-flight (TOF) is the time interval between the emission of an ultrasonic pulse and the arrival of the corresponding echo. Even, when the transducers are associated in more complex sensorial structures to collect more details from the environment, they are often able to emit and receive: in most cases, emission and reception are simultaneous in all the transducers of the array [8–11].

The use of the same transducer as a transmitter and as a receiver implies that the emission is coupled to the reception circuit, saturating it. This is the reason why the reception modules are usually disabled during the emission interval. Nevertheless, this disabling period does not allow the reception of echoes coming from the area close to the transducer, since their arrival is overlapped with the coupled emission, and indeed, disabled. This near area is often called the blind zone [12].

This problem is even more important if encoding techniques are used in the ultrasonic emission [13]. These techniques consist of the usage of a binary code with good auto-correlation properties. The ultrasonic emission is coded by this sequence, so a correlation process should be computed in the reception for the determination of the TOF. This provides more accurate measurements, with a higher immunity to noise. But, on the other hand, the length of the binary code determines the duration of the emission process and, therefore, the dimension of the blind zone.

Previous works have used different types of binary sequences: Barker codes [6,14], pseudo-random sequences [8,10] or Golay complementary pairs [11,15]. In all cases, the dimension of the blind zone depends, not only on the sequence length, but also on the kind of modulation used to adapt the sequence to the transducer's features. Different proposals usually find a commitment between accuracy and immunity (by increasing the sequence length) and the dimension of the blind zone.

* Corresponding author. Tel.: +34 9188 56583; fax: +34 9188 56591.
E-mail addresses: alvaro@depeca.uah.es (Á. Hernández), urena@depeca.uah.es (J. Ureña), mazo@depeca.uah.es (M. Mazo), Jesus@depeca.uah.es (J.J. García), ajimenez@depeca.uah.es (A. Jiménez), Fernando@depeca.uah.es (F.J. Álvarez).

0924-4247/$ – see front matter © 2006 Elsevier B.V. All rights reserved.
doi:10.1016/j.sna.2006.03.008

In previous works using encoding techniques, the blind zone dimension (d_b) increases according to the sequence length, and the modulation features. As an example, in Refs. [6,14] this size was around 17 cm for a 13-bit Barker code with a Binary Phase Shift Keying (BPSK) modulation. On the other hand, in those applications where no encoding is used, the ultrasonic emission consists of a train of pulses, whose energy bounced back is detected at the reception. The ranged distances and the precision are higher as much energy is emitted, so the number of pulses should be as high as possible. Nevertheless, more pulses imply a longer blind zone where reflectors will be not detected. In these cases, the dimension of the blind zone (d_b) reaches distances up to 5 cm [17] for trains of 16 pulses on a 50 kHz emitting signal. Summing it up, encoding techniques considerably improve the precision achieved in the TOF determination and the robustness to noise influence, but it also increases the blind zone dimension (d_b), not allowing the detection of near reflectors.

This work explains how a novel encoding technique, based on Golay complementary pairs, can be used to reduce the blind zone to negligible distances, by taking advantage of the particular auto-correlation features of Golay pairs. Section 2 deals with the different binary sequences used in ultrasonic encoding and describes the processing algorithm here proposed. Section 3 shows some real results of detection in the blind zone with the developed system. Finally, some conclusions are discussed in Section 4.

2. Ultrasonic emission encoding

There are numerous binary sequences that can be used for encoding of the ultrasonic emission: 13-bit Barker code [5,6,4], pseudo-random PN sequences [8,10], Gold codes [18,19] or Golay complementary pairs [20,21].

The blind zone is caused by the coupling of the emitted signal in the reception stages, so, during the emission interval, the received echoes are overlapped with the coupled emission. This implies that it is not possible to receive these echoes completely, since the reception circuits are usually either saturated or disabled.

In these cases, it is remarkable to analyse how the auto-correlation functions for different sequences change according to the loss of bits at their beginning. Typically, the loss of bits implies the increase in the sidelobes of the auto-correlation function and a decrease in the mainlobe: the higher the loss is, the higher the sidelobes are compared to the mainlobe. The sidelobe-to-mainlobe ratio (SMR) is here used to depict suitably this behaviour. In ideal conditions, sidelobes should be null or negligible; nevertheless, a high SMR implies remarkable sidelobes, with amplitudes similar to the mainlobe, so the detection of echoes and the accuracy can be constrained, even not being possible to determine TOFs.

As a comparative analysis, Fig. 1 shows the behaviour of PN sequences under these conditions for different lengths, whereas Fig. 2 does the same for Gold codes. It is interesting to observe that SMR ratio improves for longer sequences in both cases. These results are compared to those for Golay complementary pairs in next section.

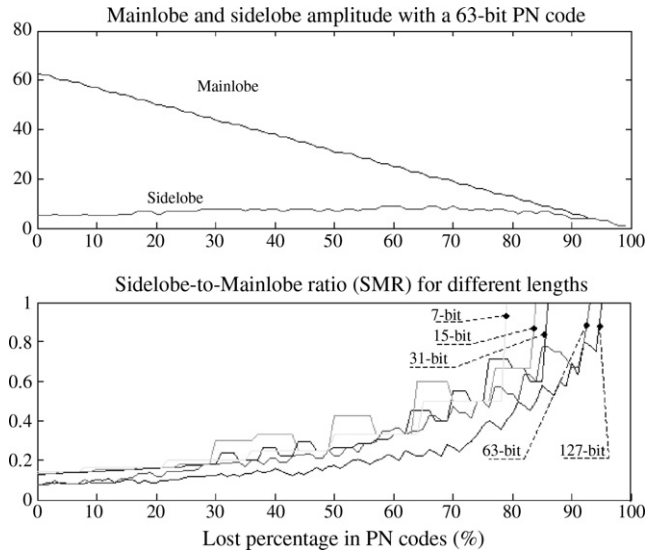

Fig. 1. Behaviour of PN sequences when loosing a percentage of the sequence.

2.1. Golay complementary pairs

This work has been focused on a pair of Golay complementary sequences [20,22] whose feasibility in ultrasonic systems to determine TOFs has been shown in previous works [21,23]. This pair is composed of two sequences, $A[n]$ and $B[n]$, where the addition of both independent auto-correlation functions provides an ideal signal according to Eq. (1).

$$C_{AA}[n] + C_{BB}[n] \begin{cases} 2N & n = 0 \\ 0 & n \neq 0 \end{cases} \quad (1)$$

where $A[n]$ and $B[n]$ are the sequences with values in $\{-1, +1\}$, N the number of bits, or the length of sequences and C_{AA} $[n]$ C_{BB} $[n]$ are the auto-correlation functions of both sequences, $A[n]$ and $B[n]$, respectively. Fig. 3 shows the result of this process for a 32-bit Golay complementary pair. Two cases are considered.

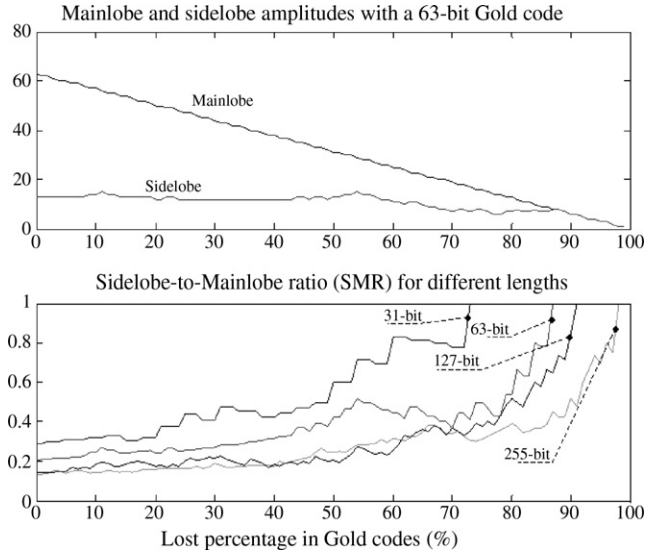

Fig. 2. Behaviour of Gold codes when loosing a percentage of the sequence.

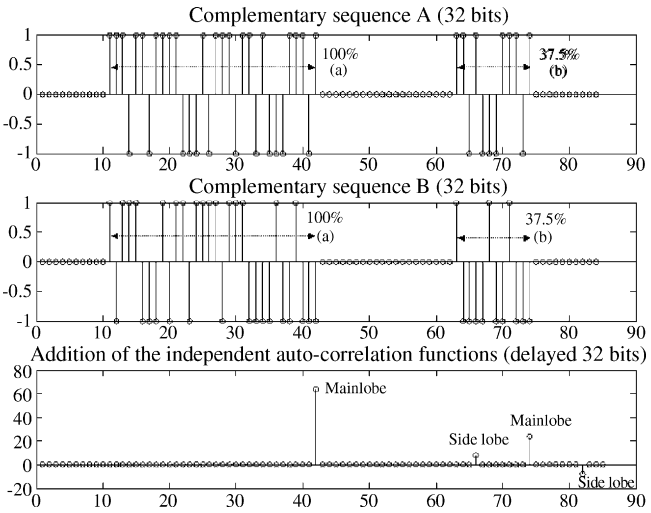

Fig. 3. Example of an auto-correlation function for a 32-bit Golay complementary pair. Two cases are described: (a) the whole sequences are received; (b) the beginning of the sequences is lost (only 37.5% is considered).

The case (a) describes the arrival of the whole sequences, so only the mainlobe is obtained and no sidelobes appear. On the other hand, in the case (b), the beginning is lost and only 37.5% of the sequences are processed; now the mainlobe amplitude decreases and sidelobes are not null. The SMR is zero in the first case, whereas it increases for the second one. The increase of the SMR implies more difficulties to identify the mainlobe, since its amplitude is more reduced and sidelobes can have similar values.

Fig. 4 shows the behaviour of Golay complementary pairs when loosing the beginning of sequences (caused by a reflector inside the blind zone). Compared to the other codes mentioned before, it is important to remark that the SMR ratio approximately shows the same behaviour, independently of the length of the Golay pair.

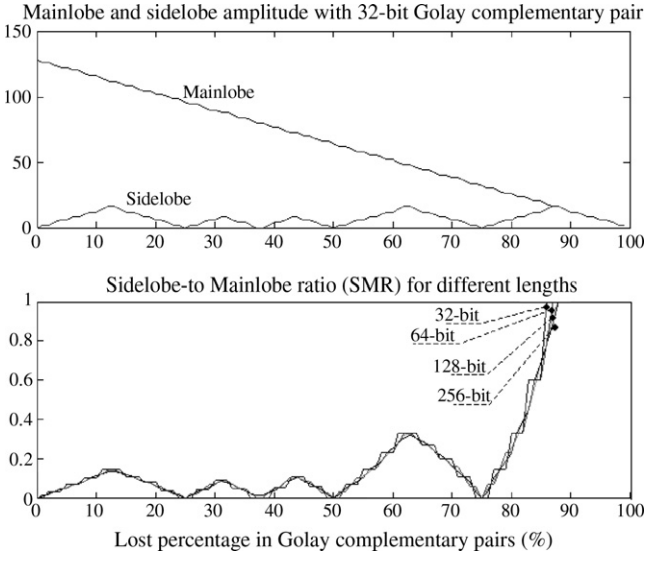

Fig. 4. Behaviour ol Golay complementary pairs when loosing a percentage of the sequence.

Table 1
Comparison of the SMR obtained for the PN, Gold and Golay sequences when loosing a percentage of the sequence

Lost percentage (%)	PN sequence	Gold code	Golay pairs
0	0.079	0.206	0
25	0.148	0.255	0
30	0.181	0.272	0.090
50	0.226	0.419	0
60	0.359	0.440	0.230
75	0.5	0.5	0
90	0.666	1.0	1.0

Table 1 summarizes SMR values for the PN, Gold and Golay codes, assuming equivalent lengths of 64 bits in all of them. As can be observed, the mainlobe can be identified more clearly in Golay complementary pairs. Table 2 shows how it is possible even to loose a 84% of the echo for a SMR of 0.5; whereas, in PN and Gold codes, percentages of 75% are only allowed for a SMR = 0.5. This implies a bigger reduction of the blind zone by using Golay complementary pairs.

2.2. The ultrasonic emission

The used ultrasonic transducer has the maximum frequency response at 50 kHz [12], therefore a modulation of the Golay sequence pair with a corresponding carrier has been carried out. A digital variant of a Quadrature Phase Shift Keying (QPSK) modulation has been used, where sequences A and B, both from the same pair of complementary sequences, have been associated to components I and Q in the modulation, respectively [11,21]. The N-bit Golay pair is obtained according to the Efficient Golay Generator (EGG) scheme proposed by Refs. [24,25] using a seed W with s bits, where $2^s = N$. The Golay pairs generated by means of the EGG structure have some particular features, which can be used to simplify the correlation process afterwards. Eq. (2) describes this modulation process, to obtain the signal $e_i[n]$ emitted by a generic transducer i.

$$\begin{aligned} e_i[n] &= A_i[n] \times S_I[n] + B_i[n] \times S_Q[n] \\ &= \sum_{k=0}^{N\cdot M\cdot m-1} A_i\left[\frac{k}{M\cdot m}\right] S[n-k] \\ &\quad + \sum_{k=0}^{N\cdot M\cdot m-1} B_i\left[\frac{k}{M\cdot m}\right] S\left[\left(N-\frac{M}{4}\right)-k\right] \end{aligned} \tag{2}$$

where M is the number of samples per period of the symbol $S[n]$ (related to the sampling frequency fs of the received signal), m the number of periods per symbol and N is the number of bits or the sequence length. The signals $A_i[n]$ and $B_i[n]$ constitute the Golay pair assigned to the emitter i. On the other

Table 2
Loss detected for the PN, Gold and Golay sequences, when assuming SMR = 0.5.

PN sequence (%)	Gold code (%)	Golay pairs (%)
75	75	84

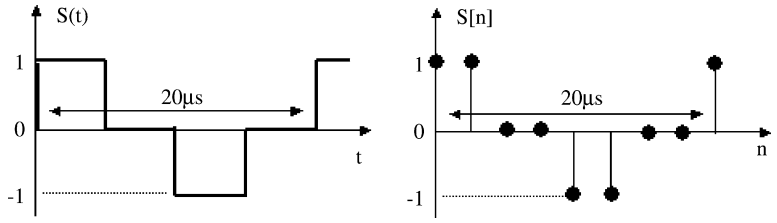

Fig. 5. Symbol $S[n]$ used in the QPSK modulation.

hand, the signals $S_I[n]$ and $S_Q[n]$ are the carriers of components I and Q, obtained from the symbol $S[n]$ with the corresponding delay. As described previously, the symbol allows to focus the emission at a frequency f_e of 50 kHz; a sampling frequency f_s of 400 kHz has been fixed, with enough oversampling to have suitable results. Because of that, $M=8$ and $m=2$ have been configured. The selected value for M allows to recover correctly the emitted signal. Whereas, the parameter m is related to the energy used for every emission and the bandwidth. The symbol $S[n]$ can be represented as a sequence, according to Eq. (3). Fig. 5 depicts a period of this carrier, once sampled at $f_s=400$ kHz.

$$
\begin{aligned}
S[n] &= [\,1 \quad 1 \quad 0 \quad 0 \quad -1 \quad -1 \quad 0 \quad 0 \quad 1 \quad 1 \quad 0 \quad 0 \quad -1 \quad -1 \quad 0 \quad 0\,] \\
S_I[n] &= [\,1 \quad 1 \quad 0 \quad 0 \quad -1 \quad -1 \quad 0 \quad 0 \quad 1 \quad 1 \quad 0 \quad 0 \quad -1 \quad -1 \quad 0 \quad 0\,] \\
S_Q[n] &= [\,0 \quad 0 \quad -1 \quad -1 \quad 0 \quad 0 \quad 1 \quad 1 \quad 0 \quad 0 \quad -1 \quad -1 \quad 0 \quad 0 \quad 1 \quad 1\,] \\
S_Q[n] &= S_I[n-2]
\end{aligned}
\tag{3}
$$

2.3. Correlating Golay complementary pairs

Once emitted the signal $e_i[n]$ by the corresponding transducer i, it travels through the environment, bouncing back to transducers from possible obstacles. In order to accurately determine the ultrasonic TOFs, it is necessary to carry out a continuous searching of possible echoes in the signal captured by a transducer. For that reason, the first step in the reception process consists of the demodulation of the received signal in order to extract the components $I_i[n]$ and $Q_i[n]$ from the signal $r_i[n]$ received by transducer i, according to Eq. (4). The signal $S[n]$ is still the modulation symbol.

$$
\begin{aligned}
I_i[n] &= C_{rS_I}[n] = r_i[n] \times S_I[n] \\
&= \sum_{k=0}^{N\cdot M\cdot m-1} r_i[k+n]S[k] \quad Q_i[n] = C_{rS_Q}[n] \\
&= r_i[n] \times S_Q[n] = \sum_{k=0}^{N\cdot M\cdot m-1} r_i[k+n]S\left[k-\frac{M}{4}\right]
\end{aligned}
\tag{4}
$$

Analysing the symbols for every component, $S_i[n]$ and $S_Q[n]$, shown in Eq. (3), it can be observed that the two necessary correlations to obtain components $I_i[n]$ and $Q_i[n]$ are redundant, as both symbols are equal, apart from a displacement of two samples (actually $M/4$ samples). For that reason, the demodulation process can be reduced to a single correlation, that allows to obtain the component $Q_i[n]$, keeping in mind that $I_i[n]$ can be obtained from the previous one by means of a $M/4$-sample delay. It is important to remark that this simplification is only possible thanks to the features of the used symbol $S[n]$: it has $M/4$ null samples at the end of every half-period see Eq. (3).

Once obtained the signals $I_i[n]$ and $Q_i[n]$ the following step is to carry out the searching of Golay sequences, each one of them in its corresponding component. This operation could be carried out by means of a classical correlation, what would allow to detect the emitted pair. Nevertheless, an optimized method, called Efficient Golay Correlator (EGC) [24,25], has been used to improve performances and resource requirements. This model allows to simplify the detection process, whenever Golay sequences with a length N power of 2 are used ($N=2^s$, where s is the number of bits of the sequence seed W, such that $W=[w_0, w_1, \ldots, w_{s-1}]$). The block diagram in Fig. 6 shows this algorithm.

Where D_s means a delay module $D_s=2^{P_s}$ is any permutation of the numbers 0, 1,. . ., $s-1$; $C_{rA}[n]$ and $C_{rA}B[n]$ are the results of the correlation between the input signal $r[n]$ and the pair of Golay sequences A and B, generated using the seed $W=[w_0, w_1, \ldots, w_{s-1}]$. These results are added and analysed to detect the received echoes.

The scheme can be adapted easily to the proposed algorithms; if a demodulation component, $I_i[n]$ or $Q_i[n]$) is applied to the EGC input, the correlation results between this component and the sequences $A_i[n]$ and $B_i[n]$ are obtained at the output. Only the in-quadrature component $Q_i[n]$ is computed. This compo-

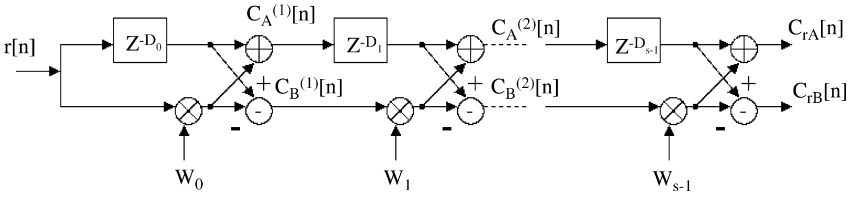

Fig. 6. Block diagram of the Efficient Golay Correlator (EGC).

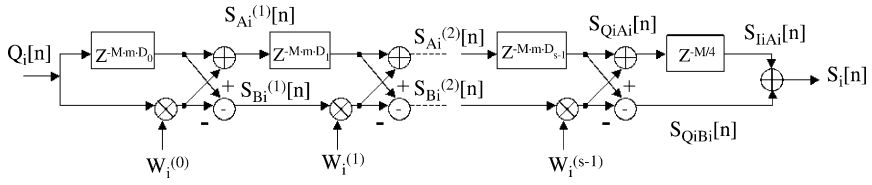

Fig. 7. Modified block diagram of the Efficient Golay Correlator (EGC).

nent becomes the input of the EGC correlator, in such a way that, at the output, the result of the correlation of the component $Q_i[n]$ by the sequence $A_i[n]$ is obtained at the top branch, $S_{Q_i A_i}[n]$, and by the sequence $Bi[n]$ at the bottom one, $S_{Q_i B_i}[n]$. The sequence $A_i[n]$ should be actually correlated by the component $I_i[n]$. The best solution consists of introducing a delay at the output of the top branch of the EGC. The result of the top branch is stored for $M/4$ cycles in order not to be used until its homologous from the bottom branch is available. In this way, the signal $S_{I_i A_i}[n]$ is obtained, and added to $S_{Q_i B_i}[n]$, providing the final signal of the process $s_i[n]$. Fig. 7 shows this adaptation using the general EGC scheme, where it can be also observed that delays D appear multiplied by a factor $M \cdot m$ ($M=8$, $m=2$). This factor is fixed by the decimation and by the number of periods per symbol $S[n]$ ($m=2$). The decimation is necessary in the signal after the acquisition process at a frequency $f_s = 400$ kHz, higher than the emitting one $f_e = 50$ kHz ($M=8$).

2.4. Detecting the received echoes

The purpose of this stage is the determination of the local maximum values in the processed signal $S_i[n]$, so they can be validated as echoes. There exist several algorithms for this purpose; among them, the simplest one is based on the definition of a static threshold U_e, so all the samples overcoming this level become possible candidates. These candidates will be definitively validated as echoes in those cases where there is not another higher candidate around it inside an analysis window formed by F_o samples. In this way, the possibility of validating the sidelobes in signals as echoes are avoided, since they will be discarded compared to the mainlobe. Parameters U_e and F_o are configured experimentally in order to achieve a better performance in the detection of echoes.

2.5. General processing scheme

A general block diagram of the processing for a generic transducer i can be developed. This diagram, shown in Fig. 8, depicts the different processing stages mentioned before, necessary in an emitter/receiver transducer.

The used ultrasonic transducer is a Polaroid electrostatic device, together with a 6500 series module [12]. This module has been modified to allow the input of any external signal $e_i[n]$ to be emitted.

3. Results

First of all, it should be remark that all the developments and experiments have been carried out assuming that all the reflectors are in the far field. According to Ref. [26], the boundary d_{NF} between the near and the far field is at 5.2 cm, see Eq. (5), for the Polaroid transducer [16], considering it as a plane circular piston. This implies that all the cases analysed later are included in the far field, avoiding the minimum values existing in the near field.

$$d_{NF} = \frac{a^2}{\lambda}\frac{\lambda}{4} \simeq 52\,\text{mm} \tag{5}$$

where a is the radius of the transducer (19.21 mm according to Ref. [16]) and λ the wavelength, assuming a propagation speed of ultrasound of 343.5 m/s for 20 °C and with a emission frequency $f_e = 50$ kHz.

Some experimental tests have been carried out to define a model for the whole system, including the behaviour of the Polaroid transducer [12,16], not only as emitter but also as receiver and the wave propagation effect. This model allows to estimate how the encoded emission is detected by the transducer, even for reflectors inside the blind zone. Fig. 9 shows a simple

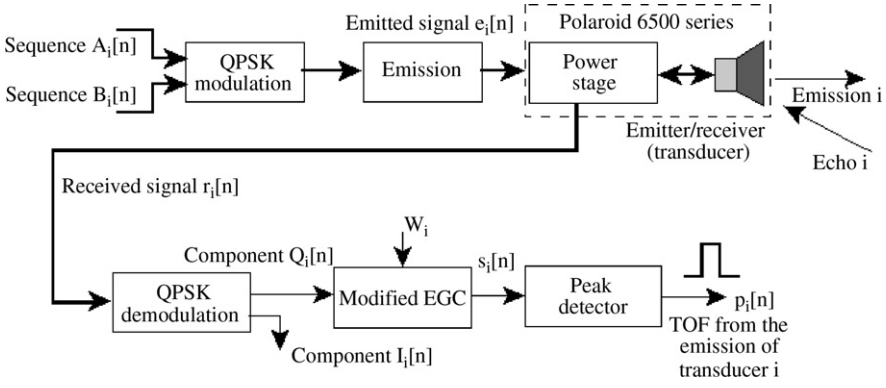

Fig. 8. Block diagram of the processing associated to a transducer i.

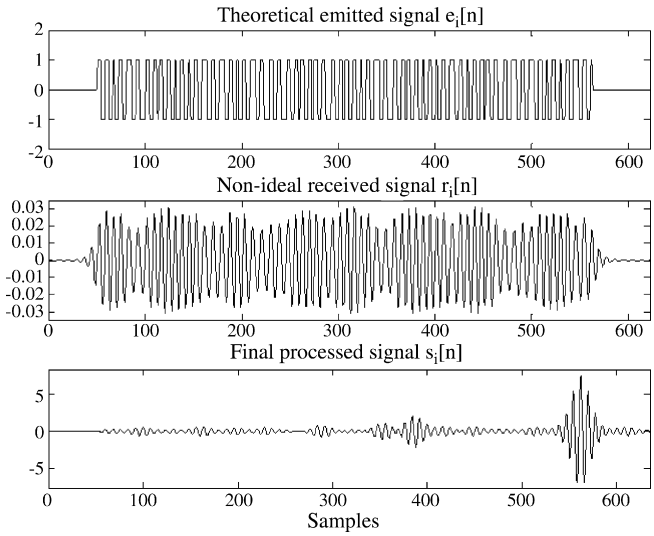

Fig. 9. Example of a 32-bit encoded emission for a whole reception.

example, based on 32-bit Golay complementary pair encoding, where the whole echo is received and processed, assuming the models for the transducer and the wave propagation.

Similar tests can be done assuming that a part of the sequence is lost. In that way, Fig. 10 shows the resulting signal when the initial 54.04% of the emitted signal is lost; this case corresponds with a reflector placed at 20 cm on the axial axis of the transducer. In Fig. 11, it is also possible to observe the result when the reflector is placed at 10 cm (8.09% of the emitted signal is lost).

This feature has been also verified in a ranging ultrasonic prototype [11]. The global system has been implemented in a FPGA-based computing platform [11], with a Xilinx XCV1000E FPGA [27] and the NuDAQ-2010 acquisition card by ADLINK Technology. It allows to achieve the real-time implementation of the proposed algorithms, by processing every ultrasonic emission before carrying out the following. It is based on the processing scheme mentioned before, assuming the following parameters: $N=32$, $m=2$ and $M=8$, for a sampling frequency of $f_s=400$ kHz. With these values, the dimension d_b reached by the blind zone is Eq. (6):

$$d_b = \frac{N \cdot m \cdot M \cdot c}{2 \cdot f_s} = 21.76\,\text{cm} \tag{6}$$

where c is the ultrasonic propagation speed. The distance d_b depends on the ultrasonic emission time t_e, which is Eq. (7):

$$t_e = \frac{N \cdot m \cdot M}{f_s} = 1.28\,\text{ms} \tag{7}$$

This emission time t_e corresponds to 512 samples, assuming a sampling frequency f_s of 400 kHz.

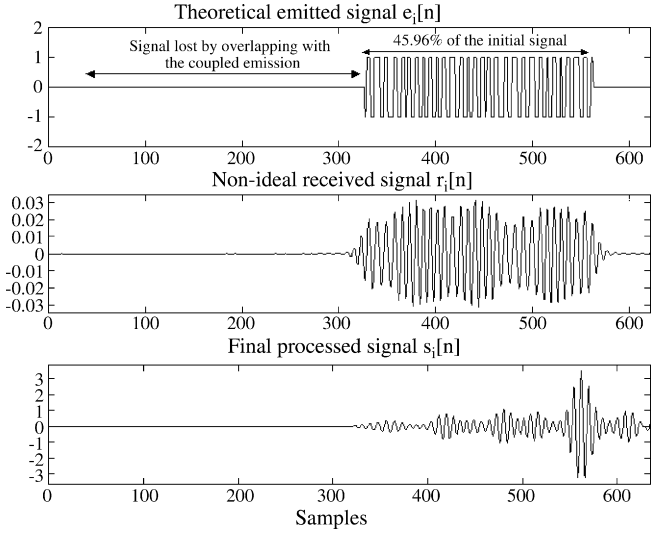

Fig. 10. Example of a 32-bit encoded emission losing the 54.04% initial echo; equivalent to a reflector placed at 20 cm.

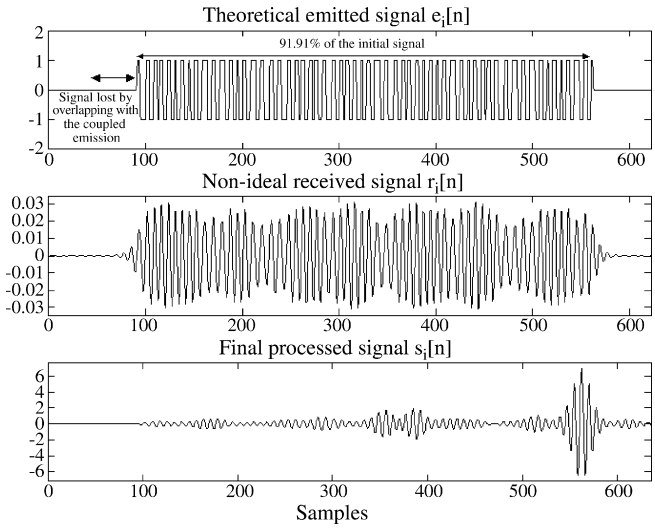

Fig. 11. Example of a 32-bit encoded emission losing the 8.09% initial echo; equivalent to a reflector placed at 10 cm.

Some tests have been carried out with an isolated emitter/receiver transducer. Some reflectors have been placed inside the blind zone, checking that it is possible to detect them by encoding the emission with Golay complementary pairs. As a first case, a pole reflector with a diameter of 9 cm was placed at a distance of 20 cm on the axial axis of the transducer. Fig. 12 shows the real signals obtained from the system. In the received signal, the presence of the coupled emission can be observed, providing the corresponding echo; but also, after finishing the emission, the reception of the first echo continues, overlapped with the coupled emission. This overlapping implies the loss of an initial part in the received echo, similar to the previous simulation in Fig. 10. It can be checked how the echo is still detected, allowing the detection of reflectors in the blind zone. Furthermore, as the reflector is so near the transducer, successive reflections happen between them providing more far echoes, always with the same distance.

A more complex case is shown in Fig. 13, where the pole obstacle has been placed at a distance of 10 cm. In this case, a higher percentage of the echo is lost overlapped with the coupled emission (equal to a loss of 54.04%, as the simulation shown in Fig. 11). Even in this case, the echo can be detected, verifying the detection inside the blind zone.

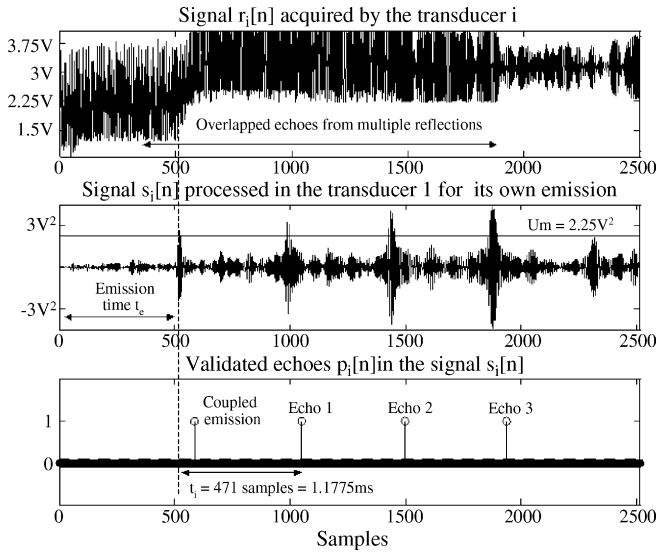

Fig. 12. Real data from a reflector placed at 20 cm (inside the blind zone) for a 32-bit codified ultrasonic emission.

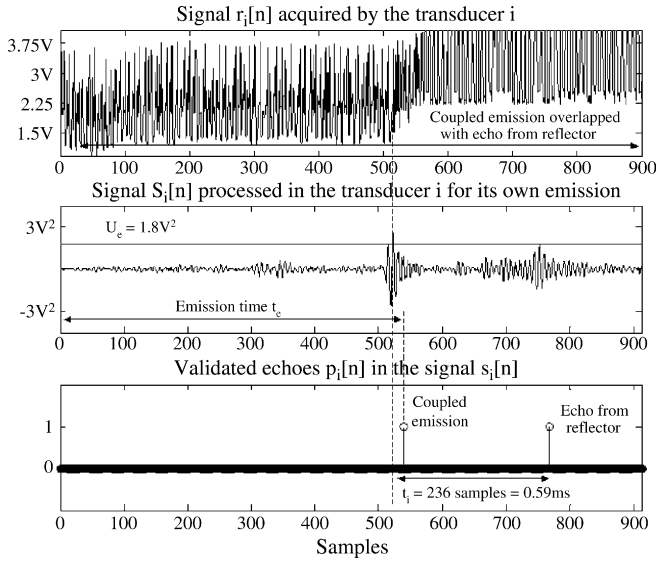

Fig. 13. Real data from a reflector placed at 10 cm (inside the blind zone) for a 32-bit codified ultrasonic emission.

Comparing the echo waveforms in Figs. 12 and 13, it is possible to observe that, the nearer the reflector is, the higher the SMR ratio becomes. Anyway, echoes in the blind zone can be easily detected since noise influence is not very high for short distances, and the reduction in the SMR ratio is not critical.

4. Conclusions

The impossibility of detecting reflectors inside the blind zone of the ultrasonic sensorial systems is one of main drawbacks presented by them. Usually, the dimension of the blind zone is determined by the length of the ultrasonic emission, since it implies a disabling interval in the reception stage that does not allow the detection of near echoes. Nevertheless, the use of binary sequences for the emission encoding provides some very interesting advantages. Apart from increasing the precision and the range, it is possible to reduce the blind zone to negligible distances, since the detection of these codes is still feasible, even when large percentages have been lost by overlapping with the coupled emission. In this work, this feature has been validated by using Golay complementary pairs and the blind zone has been reduced to almost 5 cm.

Acknowledgements

This work was supported by the Spanish Ministerio de Ciencia y Tecnología (PARMEI project, rel. DPI2003-08715-C02-01), by the University ol Alcalá (ISUAP project, ref. PI2004/033) and by the Comunidad de Madrid (ANESUS project, ref. CAM-UAH2005/016).

References

[1] J.J. Leonard, H.F. Durrant-Whyte, Mobile robot localization by tracking geometric beacons, IEEE Trans. Rob. Autom. 7 (3) (1991) 376–382.
[2] L. Kleeman, R. Kuc, Mobile robot sonar for target localization and classification, Int. J. Rob. Res. 14 (4) (1995) 295–318.
[3] A. Elfes, Sonar based real-world mapping and navigation, IEEE J. Rob. Autom. RA-3 (3) (1987) 249–264.
[4] J. Borestein, Y. Koren, Obstacle avoidance with ultrasonics sensors, IEEE J. Rob. Autom. 4 (2) (1988) 213–218.
[5] K. Audenaert, H. Peremans, Y. Kawahara, J. Van Campenhout, Accurate ranging of multiple objects using ultrasonic sensors, in: Proceedings of IEEE International Conference on Robotics and Automation, Nice, France, May, 1992, pp. 1733–1738.
[6] H. Peremans, K. Audenaert, J.M. Van Campenhout, A high resolution sensor based on tri-aural perception, IEEE Trans. Rob. Autom. 9 (1) (1993) 36–48.
[7] L. Kleeman, Advanced sonar with velocity compensation, Int. J. Robotics Res. 23 (2) (2004) 111–126.
[8] K. Jörg, M. Berg, First results in eliminating crosstalk & noise by applying pseudo-random sequences to mobile robot sonar sensing, in: Proceedings IEEE/RSJ International Conference on intelligent Robots and Systems (IROS'96), Osaka, Japan, November, 1996.
[9] L. Kleeman, Fast and accurate sonar trackers using double pulse coding, in: Proceedings of IEEE/RSJ International Conference on Intelligent Robots and Systems (IROS'99), Maui, Hawaii, November, 1999, pp. 1185–1190.
[10] S. Shoval, J. Borestein, Using coded signals to benefit from ultrasonic sensor crosstalk in mobile robots obstacle avoidance, in: Proceedings of 2001 IEEE International Conference on Robotics and Automation (ICRA'01), Seoul, Korea, May, 2001, pp. 2879–2884.
[11] A. Hernández, J. Ureña, J.J. García, M. Mazo, D. Herranz, J.P. Dérutin, J. Sérot, Ultrasonic ranging sensor using simultaneous emissions from different transducers, IEEE Trans. Ultrason. Ferroelectr. Freq. Control 51 (12) (2004) 1660–1670.
[12] Polaroid Corporation, 600 Series. Instrument grade electrostatic transducers, Technical specification, 1999.
[13] S.A. Hovanessian, Radar System Design and Analysis, Artech House Inc., Norwood, 1984.
[14] J. Ureña, M. Mazo, J.J. García, A. Hernández, E. Bueno, Correlation detector based on a FPGA for ultrasonic sensors, Microprocessors Microsyst. (23) (1999) 25–33.
[15] B.B. Lee, E.S. Furgason, High speed digital Golay code flaw detection system, Ultrasonics 21 (4) (1983) 153–161.
[16] Polaroid Corporation, Ultrasonic ranging systems, Product Specification, 1991.
[17] R. Kuc, Pseudoamplitude scan sonar maps, IEEE Trans. Rob. Autom. 17 (5) (2001) 767–770.
[18] R. Gold, Optimal binary sequences for spread spectrum multiplexing, IEEE Trans. Inf. Theory IT-13 (4) (1967) 619–621.

[19] M. Hazas, A. Ward, A novel broadband ultrasonic location system, in: Proceedings of UbiComp 2002: Ubiquitous Computing, Goteborg, Sweden, September, 2002, pp. 264–280.
[20] M.J.E. Golay, Complementary sequences, IRE Trans. Inf. Theory 7 (1961) 82–87.
[21] V. Díaz, J. Ureña, M. Mazo, J.J. García, E. Bueno, A. Hernández, Using Golay complementary sequences for multi-mode ultrasonic operation, in: Proceedings of 1999 7th IEEE International Conference on Emerging Technologies and Factory Automation (ETFA'99), Barcelona, Spain, 1999, pp. 599–604.
[22] C.C. Tseng, C.L. Liu, Complementary sets of sequences, IEEE Trans. Inf. Theory IT-18 (5) (1972) 644–652.
[23] G. Hayward, Y. Gorfu, A digital hardware correlation system for fast ultrasonic data acquisition in peak lower limited applications, IEEE Trans. Ultrason. Ferroelectr. Freq. Control 35 (6) (1988) 800–808.
[24] S.Z. Budisin, Efficient pulse compressor for Golay complementary sequences, Electron. Lett. 27 (3) (1991) 219–220.
[25] B.M. Popovic, Efficient Golay correlator, IEE Electron. Lett. 35 (17) (1999) 1427–1428.
[26] L.E. Kinsler, A.R. Prey, A.B. Coppens, J.V. Sanders, Fundamentals of Acoustics, fourth ed., John Wiley & Sons, 2000.
[27] Xilinx Inc., Virtex-E 1.8V Field Programmable Gate Arrays, Product specification, 2000.

Biographies

Álvaro Hernández obtained his electronic engineering degree from the University of Alcalá (Spain) in 1998. In 2003, he obtained his PhD from the University of Alcalá (Spain), and from the Blaise Pascal University (Prance). He is currently a lecturer of digital systems at the Electronics Department in the University of Alcalá. His research areas are multi-sensor integration, electronic systems for mobile robots, digital systems and computing architecture.

Jesús Ureña received the electronics engineering (BS) and telecommunications engineering (MS) from the Polytechnical University of Madrid (Spain) in 1986 and 1992, respectively; and his PhD degree in telecommunications from the University of Alcalá (Spain) in 1998. Since 1986, he has been a lecturer of the Electronics Department at the University of Alcalá. He has collaborated in several educational and research projects in the area of electronic control and sensorial systems for mobile robots and wheelchairs and in the area of electronic systems for railways. His current research areas are low-level ultrasonic signal processing, local positioning systems (LPS) and sensory systems for railway safety.

Manuel Mazo received his PhD degree in telecommunications in 1988, and his engineering degree (MSc) in telecommunications in 1982, all of them from the Polytechnic University of Madrid (Spain). Currently, he is a professor in the Department of Electronics at the University of Alcalá. His research areas are multi-sensor (ultrasonic, infrared and artificial vision) integration and electronic control systems applied to mobile robots and wheelchairs for physically disabled people.

Juan J. García obtained his technical telecommunication engineering degree from the University of Alcalá (Spain) in 1992, and his telecommunication engineering degree in 1998 from the University of Valencia (Spain). He has been a lecturer of analog and digital electronics in the Electronics Department of the University of Alcalá since 1994. He has worked on several public and private projects related to digital control and sensors systems, and his current areas of interest are mobile robots and multi-sensor Integration.

Ana Jiménez studied physics at the Complutense University of Madrid and material engineering at the Politecnica University of Madrid, where obtained the PhD degree in 2003. She has worked in MBE growth, fabrication and characterization of III–V nitride heterostructures for electronic applications. She joined University of Alcalá (Spain), Department of Electronics, in January 2004 as assistant professor. Currently, her research interests are focused on ultrasonic transducers, design of acquisition, analysis and processing systems for ultrasonic transducers for mobile robots.

Fernando J. Álvarez obtained his physics degree from the University of Sevilla (Spain) in 1998. He is currently an assistant professor of control engineering in the Electronics Department at the University of Extremadura. His research areas are low-level ultrasonic signal processing and the outdoor propagation of acoustic waves.